# Effect of Particle Size on Salt-Induced Diffusiophoresis Compared to Brownian Mobility

Michele S. McAfee and Onofrio Annunziata*

Department of Chemistry, Texas Christian University, Fort Worth, Texas 76129, United States

Ⓢ *Supporting Information*

ABSTRACT: For ternary polymer–salt–water systems at low polymer concentration (0.5%, w/w), we have experimentally investigated the effect of polymer size on polymer diffusiophoresis (i.e., polymer migration induced by a salt concentration gradient) and salt osmotic diffusion (i.e., salt migration induced by a polymer concentration gradient). Specifically, Rayleigh interferometry was employed to measure ternary diffusion coefficients for aqueous solutions of poly(ethylene glycol) (PEG) and KCl at 25 °C. Our investigation focused on four polymer molecular masses (from 10 to 100 kg mol^{-1}) and two salt concentrations (0.25 and 0.50 M). To describe and examine our experimental results, we introduced a

normalized diffusiophoresis coefficient as the ratio of polymer diffusiophoresis to polymer Brownian mobility. This coefficient was found to increase with polymer molecular mass, thereby demonstrating that the relative importance of polymer diffusiophoresis compared to its intrinsic Brownian mobility increases with particle size. The observed behavior was linked to preferential hydration (water thermodynamic excess) and hydration (bound water) of the macromolecule. The ratio of salt osmotic diffusion to binary salt–water diffusion approximately describes the nonuniform spatial distribution of salt along a static polymer concentration gradient at equilibrium. The significance of polymer diffusiophoresis, especially at high PEG molecular mass, was examined by considering a steady-state diffusion problem showing that salt concentration gradients can produce large enhancements and depletions of polymer concentration. This work is valuable for understanding and modeling the effect of salt concentration gradients on diffusion-based transport of polymers with applications to interfacial processes.
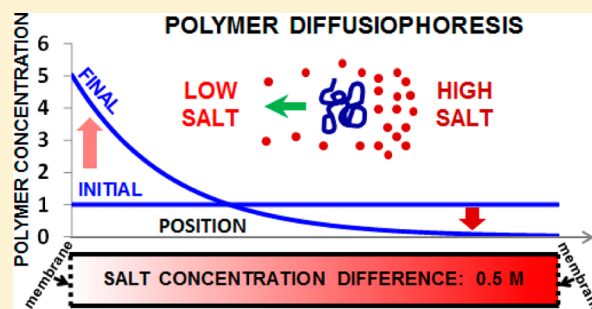
1. INTRODUCTION

Diffusion in liquids[1–3] is important in separation science,[4] phase transitions,[5] adsorption on surfaces,[6] controlled-release technologies,[7] living-system dynamics,[8] reaction kinetics,[9] pattern formation,[10] and fluid dynamics in general.[11] This transport process is particularly important for mass-transfer applications in which convection is not occurring as in the case of capillaries, transport near interfaces, and porous media.[12,13] Diffusion also plays a key role in microfluidic technologies.[14–17] One intriguing, yet not-well understood aspect of multicomponent systems is cross-diffusion.[1,17–19] This is the mechanism describing diffusion of a solute due to the concentration gradient of another solute in a multicomponent mixture.[20] For colloidal rigid particles under cosolvent concentration gradients, this phenomenon is known as diffusiophoresis.[21] This mechanism, which has been recently shown to be significant inside microfluidic devices, indicates that salt concentration gradients with tunable amplitude and direction could be used to achieve a strongly amplified particle migration, inducing either spreading or focusing of the particles in solution.[22]

Most diffusion studies on macromolecules in solutions have been performed using dynamic light scattering.[23] The measured diffusion coefficient approximately characterizes particle diffusion due to its own concentration gradient.[24,25] By

applying the theory of Brownian motion, this coefficient has been primarily used to calculate the hydrodynamic radius of the investigated particles (Stokes–Einstein equation);[26] however, dynamic light scattering cannot be used to characterize cross-diffusion. Diffusiophoresis has been characterized for large (∼100 nm) colloid particles. These studies have mainly examined how salt concentration gradients produce pressure and electrostatic gradients at the interface between a fluid and a rigid particle. The resulting forces are responsible for particle motion.[21,22] However, the use of these models in the case of macromolecules, with a large surface area accessible to solvent (e.g., polymer coils), is questionable. Here, solvation effects are expected to be relatively more complex. Furthermore, the behavior of cross-diffusion as polymer size increases is difficult to predict.

In this paper, we report the experimental characterization of cross-diffusion in aqueous KCl solutions of poly(ethylene glycol) (PEG) at several polymer molecular masses. This physicochemical investigation is important not only because it provides general insight into cross-diffusion in macromolecular systems but also because PEG is one of the most employed

hydrophilic neutral polymers for pharmaceutical and industrial applications.[13,27,28]

For a ternary polymer (1)−salt (2)−water system, diffusion can be described by the extended first law of Fick:[29]

$$-J_1 = D_{11}\nabla C_1 + D_{12}\nabla C_2 \tag{1a}$$

$$-J_2 = D_{21}\nabla C_1 + D_{22}\nabla C_2 \tag{1b}$$

where C_1 and C_2 are the molar concentrations of the macromolecule and additive, respectively, J_1 and J_2 are the corresponding molar fluxes, and the four D_{ij} values (with $i, j = 1, 2$) are the multicomponent diffusion coefficients. Main-diffusion coefficients, D_{11} and D_{22}, describe the flux of polymer and salt due to their own concentration gradients, while cross-diffusion coefficients, D_{12} and D_{21}, describe the flux of a solute due to the concentration gradient of the other solute and are responsible for coupled diffusion. Here, the cross-diffusion coefficient describing diffusion of polymer due to a salt concentration gradient (D_{12}) will be denoted as polymer diffusiophoresis. The other cross-diffusion coefficient (D_{21}), describing diffusion of salt due to a polymer concentration gradient, will be denoted as salt osmotic diffusion.

In the limit of infinitesimal polymer concentration, diffusion of polymer coils in aqueous salt mixtures is described by both the polymer tracer-diffusion coefficient, characterizing particle Brownian mobility, and polymer diffusiophoresis, characterizing particle migration parallel to the direction of a salt concentration gradient. As the polymer molecular mass increases, the polymer hydrodynamic radius increases. Thus, the corresponding tracer-diffusion coefficient decreases according to the Stokes−Einstein equation.[26] However, it is not clear how polymer diffusiophoresis correspondingly behaves. Although this cross-diffusion coefficient is expected to be proportional to its tracer-diffusion coefficient,[30] polymer preferential hydration is the driving force of polymer diffusiophoresis from high to low salt concentration.[29] This driving force is expected to approximately increase linearly with polymer molecular mass. Due the complexity of cross-diffusion phenomena, the net effect of particle mobility and preferential hydration on the dependence of diffusiophoresis on molecular mass needs to be experimentally examined. The main goal of this investigation is to determine the relative importance of polymer diffusiophoresis compared to its intrinsic Brownian mobility as a function of polymer size.

2. EXPERIMENTAL SECTION

2.1. Materials. PEG with nominal masses of 10 kg mol^{-1} (PEG10), 20 kg mol^{-1} (PEG20), and 35 kg mol^{-1} (PEG35) and poly(ethylene oxide) with a nominal mass of 100 kg mol^{-1} (PEO100) were purchased from Sigma-Aldrich and used without further purification. For PEG, certificates of analysis obtained from Sigma-Aldrich give the number (M_n) and mass (M_w) average molecular masses based on size-exclusion chromatography: $M_n = 8.39$ kg mol^{-1} and $M_w/M_n = 1.12$ for PEG10, $M_n = 18.00$ kg mol^{-1} and $M_w/M_n = 1.37$ for PEG20, and $M_n = 28.06$ kg mol^{-1} (M_w was not reported) for PEG35. For PEO100, the viscosity value of 48 cP at 25 °C was reported for a 5.0% (w/w) PEO−water solution. Mallinckrodt AR KCl with 99.9% purity was dried by heating at 450 °C for 7 h and used without further purification. Deionized water was passed through a four-stage Millipore filter system to provide high-purity water for all the experiments.

All solutions were prepared by mass with appropriate buoyancy corrections.[29] Stock concentrated solutions of PEG were made by mass to 0.1 mg. Density measurements (Mettler-Paar DMA40 density meter) were made on the stock solutions for buoyancy corrections.

The pairs of solutions for each diffusion experiment were prepared by mass. For binary PEG−water experiments, precise masses of PEG stock solutions were diluted with pure water to reach the final target PEG concentrations. For binary KCl−water solutions, precise masses of pure salt were added to flasks and diluted with pure water to reach the final target KCl concentrations. For ternary PEG−KCl−water solutions, precise masses of PEG stock solution and pure salt were added to flasks and diluted with pure water to reach the final target PEG and KCl concentrations. The densities of these solutions were measured to determine the volumetric properties and molar concentrations of the polymer (C_1/mol dm^{-3}) and salt (C_2/mol dm^{-3}). Polymer molar concentrations were based on the monomer molecular mass of 44.05 g mol^{-1}. The KCl molecular mass of 74.55 g mol^{-1} was used to calculate the salt molar concentrations.

2.2. Diffusion Experiments. Binary and ternary mutual diffusion coefficients were measured at 25.00 °C with the Gosting diffusiometer operating in the Rayleigh interferometric optical mode.[20,31] The refractive-index profile inside a diffusion cell is measured as described in ref 25 and references therein. This yields diffusion coefficients in the volume-fixed reference frame. The diffusion cell is immersed in a water bath regulated to ±0.001 °C precision and ±0.01 °C accuracy. In brief, a typical diffusion experiment starts from preparing a sharp boundary between two uniform solutions of slightly different solute concentrations located inside a vertical channel with inside width $a = 2.5$ cm. Rayleigh fringes shift horizontally as the refractive index inside the diffusion channel changes with the vertical height. This gives direct information about the refractive index, n, versus the vertical position, x. The difference in refractive index, Δn, between the two solutions is obtained from the total number of fringes, J, using $\Delta n = J\lambda/a$. We obtain refractive-index profiles at 50 different values of time, t, during the course of each experiment. The experimental refractive-index profile is then described by the normalized antisymmetric function $f(y) \equiv 2[n(y) - \bar{n}]/\Delta n$, where $y \equiv x/2\sqrt{t}$ and $0 \leq f \leq 1$. Note that the precision of a diffusion coefficient increases with the number of fringes, J. In all experiments, differences in concentration between the bottom and top solutions were chosen such that $J \approx 50$ (note that each fringe corresponds to a difference in the total concentration of solutes on the order of 0.1 g L^{-1}). Initial step-function distributions of solute concentrations were prepared with the boundary located at the center of the cell. All experimental data were obtained before detectable concentration changes occurred at the top and bottom ends of the cell, consistent with the free-diffusion boundary condition. A minimum of two experiments are required for determining the four diffusion coefficients at a given set of mean mass concentrations. These two experiments must have different combinations of solute concentration differences across the diffusion boundary. To verify reproducibility, two other duplicate experiments were performed at each set of mean concentrations. The ternary diffusion coefficients, D_{ij}, were obtained by applying the method of nonlinear least-squares as described in ref 32. Due to PEG polydispersity, a corrective procedure was applied to our ternary experiments to remove the contribution of polydispersity from the measured refractive-index profiles. This procedure, which is based on the refractive-index profiles of the corresponding binary PEG−water experiments, is described in ref 33 in detail.

3. RESULTS AND DISCUSSION

Our main goal is to examine how cross-diffusion coefficients depend on the polymer size for a ternary polymer−salt−water system at constant temperature. We will examine their behavior as a function of the salt concentration at low polymer concentration. Here, it is convenient to introduce the following two normalized cross-diffusion coefficients[30] in the solvent-fixed frame[34] (see the Supporting Information, sections S1 and S2):

$$\hat{D}_{12}(C_2) \equiv \lim_{C_1 \to 0}\left(\frac{D_{12}}{C_1} + \frac{\bar{V}_2 D_2}{1 - C_2\bar{V}_2}\right)\frac{C_2}{2y_2 D_1^0} \tag{2a}$$

$$\hat{D}_{21}(C_2) \equiv \lim_{C_1 \to 0} (D_{21} + C_2 \overline{V}_1^0 D_1^0) \frac{1}{D_2} \qquad (2b)$$

where D_1^0 and $\overline{V}_1^0$ are the polymer tracer-diffusion coefficient and infinite-dilution partial molar volume, respectively, and D_2, $\overline{V}_2$, and $y_2 = (1 + \mathrm{d}\ln y_\pm/\mathrm{d}\ln C_2)$, with $y_\pm$ being the salt mean-ionic activity coefficient, are the binary salt−water mutual-diffusion coefficient, salt partial molar volume, and nonideality thermodynamic factor, respectively. The coefficient "2" in eq 2a describes electrolyte dissociation. Since experimental diffusion coefficients are measured in the volume-fixed frame, the second term inside the parentheses of eqs 2a and 2b represents a small correction needed to convert cross-diffusion coefficients from the volume-fixed to the solvent-fixed frame.[34] Note that D_2 is defined with respect to the volume-fixed frame, while D_1^0 is independent of the employed reference frame.

Equation 2a describes polymer diffusiophoresis normalized with respect to its Brownian diffusion. This definition can be appreciated by considering the diffusion-based motion of a polymer coil in the presence of a salt concentration gradient. Here, eq 1a can be rewritten in the following way (see the Supporting Information, section S3):

$$-u_1 = D_1^0 (\nabla \ln C_1 + \hat{D}_{12} \nabla \ln a_2^{\ 2}) \qquad (3)$$

where $u_1 = J_1/C_1$ is the net polymer diffusion rate with respect to solvent and a_2 is the salt thermodynamic activity. Equation 3 shows that $\hat{D}_{12}$ represents a proportionality constant between u_1 and both the salt thermodynamic driving force, $2\nabla \ln a_2$, and D_1^0, describing the intrinsic Brownian mobility of the polymer coil. The higher the $\hat{D}_{12}$, the stronger the contribution of polymer diffusiophoresis compared to D_1^0.

Equation 2b describes normalized salt osmotic diffusion.[30] This definition can be appreciated by considering the limiting case of $D_1^0/D_2 = 0$, which is the appropriate reference condition for ternary aqueous systems containing macromolecules and relatively fast diffusing species such as small ions or osmolytes. In the limit of $D_1^0/D_2 = 0$, a macromolecule concentration gradient can be regarded as fixed within the time it takes for salt to diffuse and equilibrate along ∇C_1. After salt equilibration is achieved, the diffusion rate of salt relative to water vanishes; i.e., $J_2 = 0$ in the solvent-fixed reference frame. According to eq 1b, we can therefore write (see the Supporting Information, section S4)

$$\lim_{D_1^0/D_2 \to 0} \hat{D}_{21} = -\left(\frac{\partial C_2}{\partial C_1} \right)_{a_2} \qquad (4)$$

Thus, $\hat{D}_{21}$ is essentially a thermodynamic quantity describing the isothermal nonuniform spatial distribution of salt corresponding to its uniform chemical potential.

3.1. Polymer Binary Diffusion Coefficients.

To determine the polymer tracer-diffusion coefficient, D_1^0, we have measured the binary diffusion coefficients for polymer−water systems, D_1, as a function of the polymer concentration, C_1. Note that there are several studies on PEG diffusion coefficients and D_1^0.[35−38] However, physicochemical properties may vary among polymer samples associated with the same nominal molecular masses. Thus, it is necessary to determine D_1^0 for our specific PEG samples. Our experimental results are reported in Table 1. The values of D_1^0 are obtained from the linear extrapolation of the binary diffusion data as shown in Figure 1A for the four polymer cases. In Figure 1B, the corresponding normalized diffusion coefficients, D_1/D_1^0, are

Table 1. Binary Diffusion Coefficients, D_1, of the Polymer−Water System

| C_1/mol dm^{-3}	$D_1/10^{-9}$ m^2 s^{-1}			
	PEG10	PEG20	PEG35	PEO100
0.0413		0.05886		
0.0590	0.09576		0.04458	0.03303
0.0681	0.09641			
0.0782		0.05969		
0.0908	0.09779		0.04639	0.03566
0.1135	0.09844		0.04775	0.03724
0.1179		0.06143		
0.1405				0.04010
0.1816			0.05115	
0.2268		0.06589		

plotted as a function of the polymer volume fraction, $\phi_1 = C_1\overline{V}_1^0$, where $\overline{V}_1^0 = 0.368$ dm^3 mol^{-1} was extracted from our density measurements (value calculated on the basis of the monomer molecular mass; specific volume 0.835 cm^{3}g^{-1}). This figure shows that the slope of D_1/D_1^0 increases with the polymer molecular mass, in agreement with the literature.[35] This behavior is related to the corresponding increase in polymer−polymer repulsive net interactions.[35,39,40] Indeed, the second virial coefficient for PEG in water is positive at 25 °C and is known to increase with polymer size, as expected for polymer coils in good solvents.[39] The method of least squares based on $D_1 = D_1^0(1 + \alpha\phi_1)$ was applied to our experimental D_1 values. The obtained tracer-diffusion coefficients, D_1^0, and slopes, α, are reported in Table 2. Equivalent hydrodynamic radii, R_h, which were calculated by applying the Stokes−Einstein equation for a sphere[26] to D_1^0, are also included.

The dependence of D_1^0 on the salt concentration can be described by considering the corresponding viscosity dependence of the binary salt−water system according to $D_1^0(C_2) = D_1^0(0)/\eta_2^r(C_2)$,[26] where η_2^r is the known relative viscosity. This approach assumes that the polymer hydrodynamic radius can be regarded as independent of C_2. Since a previous study on PEG in aqueous KCl shows that R_h changes are expected to be about 1−2% within our experimental salt concentration range,[29] we can assume that R_h is constant. In Table 3, we report the values[41] of η_2^r at the experimental salt concentrations together with other physicochemical data[42−44] of the binary salt−water system relevant to eqs 2a and 2b. Note that the effect of KCl on water viscosity is very small.[41]

3.1.1. Ternary Diffusion Coefficients.
In Table 4, we report our experimental ternary diffusion coefficients in the volume-fixed reference frame. Values of D_{ij} were obtained at the polymer concentration of $C_1 = 0.1135$ mol dm^{-3} ($\phi_1 = 0.00418$) and two salt concentrations, 0.25 and 0.50 mol dm^{-3}. Since polymer−polymer interactions are relatively strong in the case of PEO100, D_{ij} values were also measured at $C_1 = 0.1703$ mol dm^{-3} ($\phi_1 = 0.00627$) to examine the effect of the polymer concentration on cross-diffusion coefficients.

The behavior of the polymer main-diffusion coefficient, D_{11}, at $C_1 = 0.1135$ mol dm^{-3} approximately follows that of D_1 as a function of the polymer molecular mass. Here, to describe deviations of D_{11} from D_1^0, we report $D_{11}/D_1^0(C_2)$ ratios in Table 5. These values also increase with the polymer molecular mass, consistent with the behavior of α (see Table 2).

The salt main-diffusion coefficient, D_{22}, was found to be 1.5% lower (see Table 5) than the corresponding binary value, D_2, at $C_1 = 0.1135$ mol dm^{-3}, independent of the polymer molecular
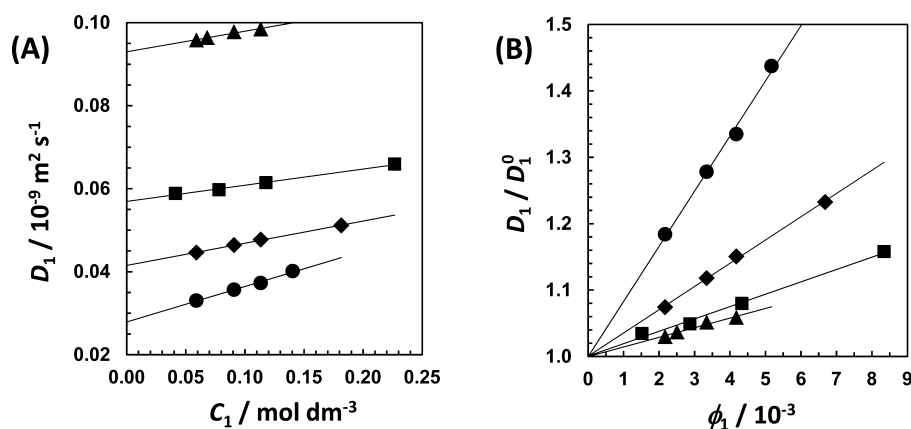
Figure 1. (A) Diffusion coefficient, D_1, for binary polymer−water systems (PEG10, triangles; PEG20, squares; PEG35, tilted squares; PEO100, circles) as a function of the polymer concentration, C_1. Solid lines are linear fits through the data. (B) Normalized diffusion coefficients, D_1/D_1^0, as a function of the polymer volume fraction, ϕ_1.

Table 2. Parameters Extracted from Binary Diffusion Coefficients, D_1

	PEG10	PEG20	PEG35	PEO100
$D_1^0/10^{-9}$ m^2 s^{-1}	0.0930 ± 0.0005^a	0.0569 ± 0.0003	0.0415 ± 0.0002	0.0279 ± 0.0005
α/mol^{-1} dm^3	14 ± 2	19 ± 1	35 ± 1	83 ± 6
R_h/nm	2.638 ± 0.006	4.311 ± 0.005	5.911 ± 0.005	8.793 ± 0.019

^{a}Uncertainties are standard deviations obtained by applying the method of least squares.

Table 3. Transport and Thermodynamic Parameters of the KCl−Water System

C_2/mol dm^{-3}	η_2^r	y_2	$D_2/10^{-9}$ m^2 s^{-1}	$\bar{V}_2$/dm^3 mol^{-1}
0.25	0.9992	0.960	1.837	0.0313
0.50	0.9978	0.892	1.847	0.0289

mass and salt concentration. This small reduction can be attributed to an obstruction effect due to the presence of polymer coils and can be described by the linear equation $D_{22}/D_2 = 1 - \beta\phi_1$, where $\beta = 3.6$ characterizes the observed obstruction effect. This β value also accurately describes the ratio $D_{22}/D_2 = 0.977$ obtained for PEO100 at $C_1 = 0.1703$ mol dm^{-3}. To gain physical insight into the determined value of β, we apply a model describing the obstructed diffusion of small particles in the presence of large hard spheres.[45] Note that this model predicts that the obstruction effect is independent of the hard-sphere size, consistent with our findings. In our case, we assume that the obstruction effect is caused by *hydrated* polymer chains with a molar volume of $\bar{V}_1^0 + \nu_0^{obs}V_0^*$, where ν_0^{obs} is the hydration number per monomer evaluated from the obstruction effect and $V_0^* = 0.01807$ dm^3 mol^{-1} is the molar

volume of pure water.[46] It is worth mentioning that this expression for the hydrated polymer volume is valid even if partial molar volumes do not correspond to the actual molar volumes of polymer and water inside the hydration layers (see the Supporting Information, section S5). According to the obstruction model, we can write $\beta = 1.5(1 + \nu_0^{obs}V_0^*/\bar{V}_1^0)$. This yields $\nu_0^{obs} = 2.9$, independent of the polymer molecular mass. This value is in agreement with hydration numbers previously reported for PEG in water.[47]

We now examine the behavior of the two cross-diffusion coefficients also reported in Table 4, the main focus of this investigation. According to these data, both D_{12} and D_{21} at $C_1 = 0.1135$ mol dm^{-3} are positive and can be approximately described as independent of the polymer molecular mass. Furthermore, D_{12} is independent of the salt concentration, while D_{21} values at $C_2 = 0.50$ mol dm^{-3} were found to be 2-fold larger than those at $C_2 = 0.25$ mol dm^{-3} within the experimental error. The latter result is consistent with the limiting condition of $D_{21} = 0$ at $C_2 = 0$.[48]

In the limit of infinitesimal polymer concentration, D_{12} becomes directly proportional to C_1, and D_{21} independent of C_1.[48] These two properties were examined in the case of

Table 4. Ternary Diffusion Coefficients, D_{ij}, of the Polymer−Salt−Water System at $C_1 = 0.1135$ mol dm^{-3}

| polymer	C_2/mol dm^{-3}	$D_{11}/10^{-9}$ m^2 s^{-1}	$D_{12}/10^{-9}$ m^2 s^{-1}	$D_{21}/10^{-9}$ m^2 s^{-1}	$D_{22}/10^{-9}$ m^2 s^{-1}
PEG10	0.25	0.0930 ± 0.0002	0.022 ± 0.002	0.040 ± 0.001	1.808 ± 0.002
PEG10	0.50	0.0938 ± 0.0002	0.026 ± 0.002	0.074 ± 0.002	1.818 ± 0.002
PEG20	0.25	0.0603 ± 0.0001	0.025 ± 0.001	0.036 ± 0.001	1.809 ± 0.002
PEG20	0.50	0.0612 ± 0.0001	0.024 ± 0.001	0.069 ± 0.001	1.816 ± 0.002
PEG35	0.25	0.0481 ± 0.0001	0.019 ± 0.003	0.033 ± 0.001	1.817 ± 0.006
PEG35	0.50	0.0489 ± 0.0001	0.024 ± 0.002	0.069 ± 0.003	1.818 ± 0.002
PEO100	0.25	0.0373 ± 0.0001	0.025 ± 0.002	0.045 ± 0.005	1.810 ± 0.002
PEO100	0.50	0.0380 ± 0.0002	0.024 ± 0.002	0.084 ± 0.005	1.818 ± 0.004
PEO100^a	0.50	0.0418 ± 0.0001	0.035 ± 0.003	0.082 ± 0.004	1.805 ± 0.005

^{a}Data obtained at $C_1 = 0.1703$ mol dm^{-3}.

Table 5. Parameters Extracted from Ternary Diffusion Coefficients, D_1

	PEG10	PEG20	PEG35	PEO100
$D_{11}\eta_2^r/D_1^{0a}$	1.00 ± 0.01	1.07 ± 0.01	1.17 ± 0.01	1.35 ± 0.03
D_{22}/D_2^a	0.984 ± 0.001	0.984 ± 0.002	0.986 ± 0.005	0.985 ± 0.001
$b_{12}/\text{mol}^{-1}\ \text{dm}^3$	1.55 ± 0.07	2.59 ± 0.06	3.19 ± 0.16	5.15 ± 0.20
$b_{21}/\text{mol}^{-1}\ \text{dm}^3$	0.085 ± 0.002	0.078 ± 0.001	0.076 ± 0.003	0.093 ± 0.003

^{a}Average between values at $C_2 = 0.25$ and 0.50 mol dm^{-3}.
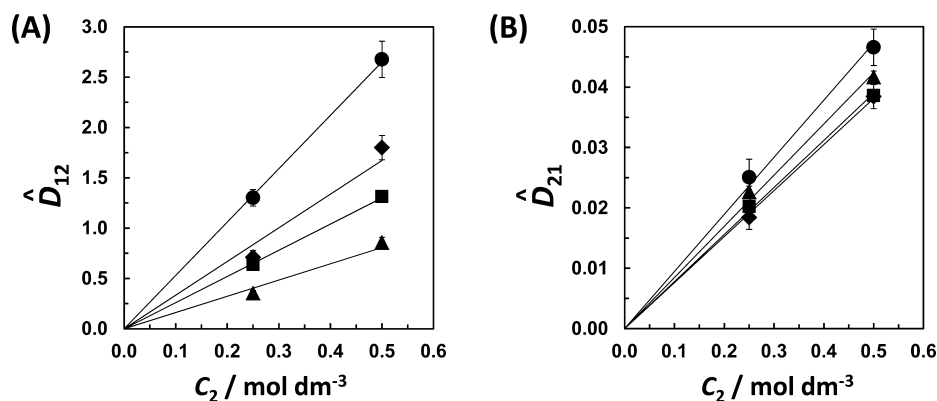
Figure 2. (A) Normalized polymer diffusiophoresis, $\hat{D}_{12}$, as a function of the salt (KCl) concentration, C_2 (PEG10, triangles; PEG20, squares; PEG35, tilted squares; PEO100, circles). Solid lines are linear fits through the data with zero intercept. (B) Normalized salt osmotic diffusion, $\hat{D}_{21}$, as a function of C_2.

PEO100 at the experimental C_1 because the corresponding polymer−polymer interactions are significant at high molecular masses. For PEO100, an increase of 50% in C_1 yielded a corresponding increase in D_{12} of 46% and a change in D_{21} of only 2%. This result, which implies that polymer−polymer interactions do not appreciably affect D_{12} and D_{21}, can be understood by considering irreversible thermodynamics.[49] In thermodynamics, polymer−polymer interactions are described by the derivative $\mu_{11} \equiv (\partial \mu_1/\partial C_1)_{C_2}$, where μ_1 is the polymer chemical potential. According to irreversible thermodynamics, this chemical-potential derivative will explicitly enter into the expressions of D_{11} and D_{21} but not those of D_{12} and D_{22}.[34] Moreover, in the case of D_{21}, the weight of μ_{11} is proportional to D_1^0/D_2. This ratio is generally small for macromolecules and decreases with the polymer molecular mass (see the Supporting Information, section S2, for more details). Hence, according to our experimental results and theoretical considerations, we can assume that the obtained values of cross-diffusion coefficients at finite polymer concentration adequately describe, within the experimental error, the behavior of cross-diffusion in the limit of infinitesimal polymer concentration. Similar results were also obtained for lysozyme−NaCl−water systems.[30] Thus, our cross-diffusion coefficients in Table 3 were used together with the physicochemical parameters in Tables 1 and 3 to calculate polymer diffusiophoresis ($\hat{D}_{12}$) and salt osmotic diffusion ($\hat{D}_{21}$) according to eqs 2a and 2b. The behaviors of $\hat{D}_{12}$ and $\hat{D}_{21}$ as a function of the salt concentration are shown in Figure 2.

For neutral hydrophilic macromolecules, both coefficients are expected to be directly proportional to the salt concentration[30] and approach zero as $C_2 \rightarrow 0$ (with $C_1/C_2 = 0$):

$$\hat{D}_{12} = b_{12}C_2 \tag{5a}$$

$$\hat{D}_{21} = b_{21}C_2 \tag{5b}$$

The method of least squares based on eqs 5a and 5b was then applied, and the corresponding values of b_{12} and b_{21} are reported in Table 5. The determined coefficient b_{21} can be approximately described as independent of the polymer size, while b_{12} was found to increase with the polymer size. The latter experimental result compensates for the corresponding decrease in D_1^0 (see eq 2a).

The parameter b_{21}, as shown by eq 4, approximately describes polymer preferential hydration. Specifically, it can be shown[30,34,48] that $b_{21} \approx \overline{V}_1^0 + \nu_0^{exc}V_0^*$, where ν_0^{exc} is the excess of water molecules[50,51] per monomer (see the Supporting Information, section S5). In our case, we find that $\nu_0^{exc} \approx 3$, consistent with the hydration numbers obtained from obstruction. On the other hand, the parameter b_{12} is of more difficult interpretation. For hydrated polymers, it can be shown[30,34,48] that $b_{12} \approx n(\nu_0^{exc} - \nu_0^{hyd})V_0^*$, where ν_0^{hyd} is the number of water molecules per monomer diffusing with polymer coils and n is the degree of polymerization (see the Supporting Information, section S5). Here, polymer poly-dispersity is neglected. In our case, we find that ν_0^{hyd} is 80−90% of ν_0^{exc}. That ν_0^{hyd} is smaller than ν_0^{exc} can be understood by considering that the excess of water molecules is a thermodynamic parameter that takes into account not only water molecules strongly bound to a polymer chain but also those loosely interacting with polymer coils, which still contribute to the net depletion of salt in the local polymer domain. The observed increase of b_{12} with polymer size can be related to the corresponding increase in n. However, the dependence of $\nu_0^{exc} - \nu_0^{hyd}$ on the polymer size also needs to be taken into account to explain the experimental behavior of b_{12}. This result is still consistent with that of b_{21} and ν_0^{exc} being approximately independent of the polymer size. Although ν_0^{hyd} and ν_0^{exc} can weakly depend on the polymer size when taken separately, the corresponding dependence of the difference $\nu_0^{exc} - \nu_0^{hyd}$ may be relatively stronger because these two parameters have a similar magnitude. For example, the observed increase of b_{12} with the polymer molecular mass can be described by
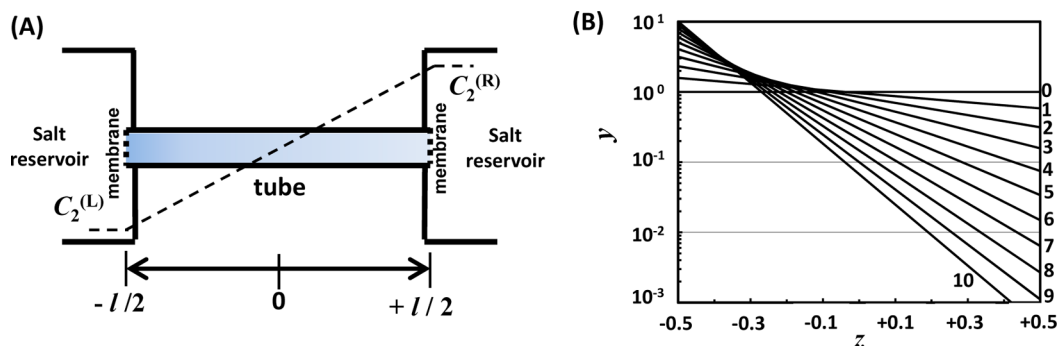
Figure 3. (A) Schematic diagram for examining the role of polymer diffusiophoresis in conditions of steady-state diffusion. A tube of length l contains a polymer solution and is connected to two salt reservoirs with salt concentrations $C_2^{(L)}$ and $C_2^{(R)}$. The dashed line with positive slope describes the salt concentration profile in steady-state conditions. The two vertical dashed lines at the tube extremities denote two membranes not permeable to the polymer component. (B) Logarithmic diagram showing normalized polymer concentration profiles, $y \equiv C_1/C_1^0$, as a function of normalized positions $z \equiv x/l$ inside the tube (solid lines) for 11 values of $\beta \equiv 2b_{12}\Delta C_2$ (numbers associated with each line).

setting ν_0^{exc} independent of n and ν_0^{hyd} directly proportional to $n^{0.1}$.

In conclusion, polymer diffusiophoresis can be satisfactorily described by considering the two hydration parameters ν_0^{hyd} and ν_0^{exc}. However, a more detailed quantitative understanding of the effect of the polymer molecular mass on $\hat{D}_{12}$ is difficult to extract from our experimental data considering that $b_{12} \approx n(\nu_0^{\mathrm{exc}} - \nu_0^{\mathrm{hyd}})V_0^*$ is an approximate description of the complex mechanism of diffusiophoresis and sample polydispersity was ignored.

3.1.2. Role of Polymer Diffusiophoresis in Steady-State Diffusion. The most important result of our experimental investigation is that $\hat{D}_{12}$ increases with the polymer molecular mass. This implies that the role of diffusiophoresis becomes more important as the polymer size increases according to eq 2a. To examine the significance of polymer diffusiophoresis, we consider steady-state diffusion occurring between two compartments separated by an intermediate section with length l representing a tube (e.g., a capillary tube or a tube filled with porous media). This tube is positioned between $x = -l/2$ and $x = +l/2$ with its two extremities capped with semipermeable membranes as shown in Figure 3A. The two tube extremities are attached to two compartments, representing two binary salt–water solutions at different salt concentrations, $C_2^{(L)}$ and $C_2^{(R)}$. These two concentrations are maintained constant so that steady-state conditions inside the tube can be achieved. If the salt diffusion coefficient can be approximated as a constant, we can write $C_2 = \overline{C}_2 + \Delta C_2(x/l)$, where $\overline{C}_2 \equiv (C_2^{(L)} + C_2^{(R)})/2$ and $\Delta C_2 = C_2^{(R)} - C_2^{(L)}$.

We now consider a uniform polymer solution embedded in this tube at the low concentration of C_1^0. Here we ignore salt osmotic diffusion because the polymer concentration is low. Since macromolecules cannot cross the two membranes, the condition $u_1 = 0$ must be respected throughout the tube in steady-state conditions. Thus, eq 3 becomes

$$\frac{\mathrm{d}\ln C_1}{\mathrm{d}\ln a_2} = -\hat{D}_{12} \tag{6}$$

If we neglect salt thermodynamic nonideality, and apply eq 5a, eq 6 can be rewritten in the following way:

$$\frac{\mathrm{d}\ln C_1}{\mathrm{d}C_2} = -2b_{12} \tag{7}$$

Integration with respect to $x = 0$ yields

$$C_1 = C_1(0)\exp(-2b_{12}\Delta C_2 x/l) \tag{8}$$

where $C_1(0)$ is the polymer concentration at $x = 0$. This concentration can be replaced by the initial uniform polymer concentration, C_1^0, using the following mass balance:

$$C_1^0 = \frac{1}{l}\int_{-l/2}^{+l/2} C_1\,\mathrm{d}x = \frac{C_1(0)}{b_{12}\Delta C_2}\sinh(b_{12}\Delta C_2) \tag{9}$$

Thus, substitution of $C_1(0)$ with C_1^0 in eq 8 yields

$$y = \frac{\beta\exp(-\beta z)}{2\sinh(\beta/2)} \tag{10}$$

where $y \equiv C_1/C_1^0$, $z \equiv x/l$, and $\beta \equiv 2b_{12}\Delta C_2$. Normalized concentration profiles $y(z)$ for several β values are shown in Figure 3B. These profiles show that the polymer concentration is enhanced and depleted near the left and right membrane locations, respectively. In the case of PEO100 and $\Delta C_2 = 0.5$ mol dm^{-3}, we have $\beta \approx 5$. As we can deduce from Figure 3B, the polymer concentration at $z = -0.5$ is predicted to be about 5-fold higher than C_1^0. On the other hand, polymer at $z = +0.5$ is predicted to be substantially depleted with a concentration that is only ~3% of C_1^0.

We believe that these diffusiophoresis effects are significant and can be exploited in diffusion-based mass-transfer processes, especially in those cases in which the Brownian motion of macromolecules is the rate-limiting step. Here, salt concentration gradients could be employed to enhance the diffusion-based transport of macromolecules. For example, diffusion of macromolecules is often the rate-determining step in the case of adsorption on surfaces.[5,6] This process is important for the preparation of functionalized surfaces for surface catalysis and sensing (e.g., surface plasmon resonance) applications.[6] Here, salt concentration gradients can be potentially used to enhance particle transport and the efficiency of adsorption processes. A hypothetical apparatus enhancing adsorption of particles by diffusiophoresis is shown in Figure 4.

3.1.3. Role of Salt Osmotic Diffusion in Thermodynamics. Here, we discuss some aspects related to salt osmotic diffusion. Although $\hat{D}_{21}$ plays a marginal role in the diffusion-based transport at low polymer concentration, this parameter is valuable because of its direct relation to polymer preferential hydration in the presence of salt. Since $\hat{D}_{21}$ is approximately a thermodynamic quantity, the examination of the physicochem-
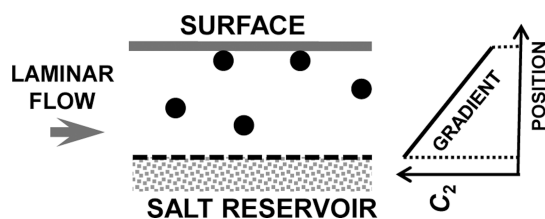
Figure 4. A solution of macromolecules (circles) flows parallel to a functionalized surface and a salt solution reservoir separated by a supported semipermeable membrane (dashed line). The induced salt gradient perpendicular to the surface enhances the adsorption kinetics.

ical behavior of $\hat{D}_{21}$ represents the first needed step toward the examination of the more complex behavior of $\hat{D}_{12}$.

Values of b_{21} extracted from $\hat{D}_{21}(C_2)$ can be used to estimate the thermodynamic properties of ternary mixtures containing macromolecules and small cosolutes. For example, they can predict salt partitioning occurring in an isothermal equilibrium-dialysis experiment. As illustrated in Figure 5, a compartment
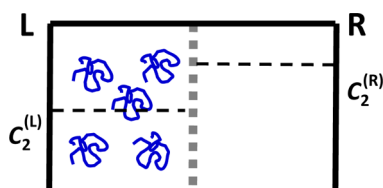
Figure 5. A compartment containing a ternary polymer−salt−water solution (L) is connected to a compartment containing a binary salt−water solution (R) through a semipermeable membrane (vertical dashed line). The two horizontal dashed lines describe the different salt concentrations, $C_2^{(L)}$ and $C_2^{(R)}$, in the left and right compartments, respectively.

containing a polymer−salt−water solution (L) is connected to a salt−water solution (R) through a semipermeable membrane. At equilibrium, we can first substitute eq 5b into eq 4, then integrate C_2 with respect to C_1, and then obtain

$$\frac{C_2^{(R)}}{C_2^{(L)}} = \exp(b_{21}C_1^{(L)}) \tag{11}$$

where $C_2^{(L)}$ and $C_2^{(R)}$ are the equilibrium salt concentrations in L and R, respectively, and $C_1^{(L)}$ is the polymer concentration in L. For PEG volume fractions of 1% and 10%, the value of $b_{21} \approx 0.08$ mol^{-1} dm^3 (see Table 5) can be used to predict a salt enrichment in R of ∼2% and ∼20%, respectively. Furthermore, as an extension of the equilibrium-dialysis problem, we observe that b_{21} can also be linked to salt partitioning between two coexisting liquid phases brought about by liquid−liquid phase separation. Similarly to eq 11, we can deduce that $\ln(C_2^{(II)}/C_2^{(I)}) \approx -b_{21}(C_1^{(II)} - C_1^{(I)})$, where the superscripts (I) and (II) denote the two coexisting phases. Thus, b_{21} values can be used to estimate the slopes of tie lines associated with liquid−liquid phase boundaries.

■ CONCLUSIONS

For ternary PEG−KCl−water systems, the role of polymer molecular mass in the behavior of the two normalized cross-diffusion coefficients, $\hat{D}_{12}(C_2)$ and $\hat{D}_{21}(C_2)$, was investigated at low C_1. Our results show that the relative importance of polymer diffusiophoresis with respect to its intrinsic Brownian mobility increases with the macromolecule size. We have

examined cross-diffusion effects by considering a steady-state diffusion problem. This showed that salt concentration gradients can produce large enhancements and depletions of polymer concentration due to diffusiophoresis. Thus, the mechanism of diffusiophoresis can be used to enhance transport of macromolecules when their Brownian mobility is low. The other cross-diffusion coefficient, salt osmotic diffusion, is essentially a thermodynamic parameter that can be used to estimate salt partitioning between two phases with different macromolecule concentrations.

■ ASSOCIATED CONTENT

ⓢ Supporting Information

Appendix containing theoretical relations relevant to this manuscript. This material is available free of charge via the Internet at http://pubs.acs.org/.

■ AUTHOR INFORMATION

Corresponding Author

*Phone: 817-257-6215. Fax: 817-257-5851. E-mail: O. Annunziata@tcu.edu.

Notes

The authors declare no competing financial interest.

■ ACKNOWLEDGMENTS

■ REFERENCES

(1) Bird, R. B. Five decades of transport phenomena. *AIChE J.* **2003**, *50*, 273−287.

(2) Curtiss, C. F.; Bird, R. B. Multicomponent diffusion. *Ind. Eng. Chem. Res.* **1999**, *38*, 2515−2522.

(3) Tyrrell, H. J. V.; Harris, K. R. *Diffusion in Liquids*; Butterworths: London, 1984.

(4) Keurentjes, J. T. F.; Janssena, A. E. M.; Broeka, A. P.; Van der Padta, A.; Wesselingh, J. A.; Van 'T Riet, K. Multicomponent diffusion in dialysis membranes. *Chem. Eng. Sci.* **1992**, *47*, 1963−1971.

(5) Petsev, D. N.; Chen, K.; Gliko, O.; Vekilov, P. G. Diffusion-limited kinetics of the solution-solid phase transition of molecular substances. *Proc. Natl. Acad. Sci. U.S.A.* **2003**, *100*, 792−796.

(6) Gedik, E. T. Surface chemistry in SPR technology. In *Handbook of Surface Plasmon Resonance*; Schasfoort, R. B. M., Tudos, A. J., Eds.; Royal Chemical Society: Cambridge, U.K., 2008; pp 173−220.

(7) Kanjickal, D. G.; Lopina, S. T. Modeling of drug release from polymeric delivery systems. *Crit. Rev. Ther. Drug Carrier Syst.* **2004**, *21*, 345−386.

(8) Brackley, C. A.; Cates, M. E.; Marenduzzo, D. Intracellular facilitated diffusion: Searchers, crowders, and blockers. *Phys. Rev. Lett.* **2013**, *111*, 108101.

(9) Miguez, D. G.; Vanag, V. K.; Epstein, I. R. Fronts and pulses in an enzymatic reaction catalyzed by glucose oxidase. *Proc. Natl. Acad. Sci. U.S.A.* **2007**, *104*, 6992−6997.

(10) Vanag, V. K.; Epstein, I. R. Cross-diffusion and pattern formation in reaction-diffusion systems. *Phys. Chem. Chem. Phys.* **2009**, *11*, 897−912.

(11) Page, M. A. Fluid dynamics propelled by diffusion. *Nat. Phys.* **2010**, *6*, 486.

(12) Garcia-Ruiz, J. M. Counterdiffusion methods for macro-molecular crystallization. *Methods Enzym.* **2003**, *368*, 130−154.

(13) Lin, C. C.; Anseth, K. S. PEG hydrogels for the controlled release of biomolecules in regenerative medicine. *Pharm. Res.* **2009**, *26*, 631−643.

(14) Whitesides, G. M. The origin and the future of microfluidics. *Nature* **2006**, *442*, 368−373.

(15) Weigl, B. H.; Yager, P. Microfluidics: Microfluidic diffusion-based separation and detection. *Science* **1999**, *283*, 346−347.

(16) Atencia, J.; Beebe, D. J. Controlled microfluidic interfaces. *Nature* **2005**, *437*, 648−655.

(17) Dror, I.; Amitay, T.; Yaron, B.; Berkowitz, B. Salt-pump mechanism for contaminant intrusion into coastal aquifers. *Science* **2003**, *300*, 950.

(18) Jervais, T.; Jensen, K. F. Mass transport and surface reactions in microfluidic systems. *Chem. Eng. Sci.* **2006**, *61*, 1102−1121.

(19) Schurr, J. M.; Fujimoto, B. S.; Huynh, L.; Chiu, D. T. A theory of macromolecular chemotaxis. *J. Phys. Chem. B* **2013**, *117*, 7626−7652.

(20) Albright, J. G.; Annunziata, O.; Miller, D. G.; Paduano, L.; Pearlstein, A. J. Precision measurements of binary and multi-component diffusion coefficients in protein solutions relevant to crystal growth: Lysozyme chloride in water and aqueous NaCl at pH 4.5 and 25 °C. *J. Am. Chem. Soc.* **1999**, *121*, 3256−3266.

(21) Keh, H. J.; Anderson, J. L. Colloid transport by interfacial forces. *Annu. Rev. Fluid Mech.* **1989**, *21*, 61−99.

(22) Abécassis, B.; Cottin-Bizonne, C.; Ybert, C.; Ajdari, A.; Bocquet, L. Boosting migration of large particles by solute contrasts. *Nat. Mater.* **2008**, *7*, 785−789.

(23) Schmitz, K. S. *Introduction to Dynamic Light Scattering by Macromolecules*; Academic Press: San Diego, CA, 1990.

(24) Sutherland, E.; Mercer, S. M.; Everist, M.; Leaist, D. G. Diffusion in solutions of micelles. What does dynamic light scattering measure? *J. Chem. Eng. Data* **2009**, *54*, 272−278.

(25) Annunziata, O.; Buzatu, D.; Albright, J. G. Protein diffusion coefficients determined by macroscopic-gradient Rayleigh interferom-etry and dynamic light scattering. *Langmuir* **2005**, *21*, 12085−12089.

(26) Tanford, C. *Physical Chemistry of Macromolecules*; Wiley: New York, 1961; p 356.

(27) Albertsson, P. A. *Partition of Cell Particles and Macromolecules*; Wiley: New York, 1986.

(28) McPherson, A. *Crystallization of Biological Macromolecules*; Cold Spring Harbor Laboratory Press: Cold Spring Harbor, NY, 1998.

(29) Tan, C.; Albright, J. G.; Annunziata, O. Determination of preferential-interaction parameters by multicomponent diffusion. Applications to the poly(ethylene glycol)−salt−water ternary mixtures. *J. Phys. Chem. B* **2008**, *112*, 4967−4974.

(30) Annunziata, O.; Buzatu, D.; Albright, J. G. Protein diffusiophoresis and salt osmotic diffusion in aqueous solutions. *J. Phys. Chem. B* **2012**, *116*, 12694−12705.

(31) Miller, D. G.; Albright, J. G. Optical methods. In *Measurement of the Transport Properties of Fluids: Experimental Thermodynamics*; Wakeham, W. A., Nagashima, A., Sengers, J. V., Eds.; Blackwell Scientific Publications: Oxford, U.K., 1991; Vol. *III*, pp 272−294.

(32) Miller, D. G. A method for obtaining multicomponent diffusion coefficients directly from Rayleigh and Gouy fringe position data. *J. Phys. Chem.* **1988**, *92*, 4222−4226.

(33) Zhang, H.; Annunziata, O. Effect of macromolecular polydispersity on diffusion coefficients measured by Rayleigh interferometry. *J. Phys. Chem. B* **2008**, *112*, 3633−3643.

(34) Zhang, H.; Annunziata, O. Macromolecular hydration compared with preferential hydration and their role on macromolecule-osmolyte coupled diffusion. *Phys. Chem. Chem. Phys.* **2009**, *11*, 8923−8932.

(35) Vergara, A.; Paduano, L.; Vitagliano, V.; Sartorio, R. Mutual diffusion in aqueous solution of poly(ethylene glycol) samples. Some comments on the effect of chain length and polydispersity. *Phys. Chem. Chem. Phys.* **1999**, *1*, 5377−5383.

(36) Vergara, A.; Paduano, L.; Mangiapia, G.; Sartorio, R. Diffusion coefficient matrix in nonionic polymer−solvent mixtures. *J. Phys. Chem. B* **2001**, *105*, 11044−11051.

(37) Waggoner, R. A.; Blum, F. D.; Lang, J. C. Diffusion in aqueous solutions of poly(ethylene glycol) at low concentrations. *Macro-molecules* **1995**, *18*, 2658−2664.

(38) Brown, W. Slow-mode diffusion in semidilute solutions examined by dynamic light scattering. *Macromolecules* **1984**, *17*, 66−72.

(39) Striolo, A.; Prausnitz, J. M. Osmotic second virial coefficient for linear and star poly(ethylene oxide). *Polymer* **2001**, *42*, 4773−4775.

(40) Hasse, H.; Kany, H.-P.; Tintinger, R.; Maurer, G. Osmotic virial coefficients of aqueous poly(ethylene glycol) from laser-light scattering and isopiestic measurements. *Macromolecules* **1995**, *28*, 3540−3552.

(41) Zhang, H.-L.; Han, S.-J. Viscosity and density of water + sodium chloride + potassium chloride solutions at 298.15 K. *J. Chem. Eng. Data* **1996**, *41*, 516−520.

(42) Miller, D. G.; Rard, J. A. Mutual diffusion coefficients of $BaCl_2$−H_2O and KCl−H_2O at 25 °C from Rayleigh interferometry. *J. Chem. Eng. Data* **1980**, *25*, 211−215.

(43) Miller, D. G. Application of irreversible thermodynamics to electrolyte solutions. I. Determination of ionic transport coefficients l_{ij} for isothermal vector transport processes in binary electrolyte systems. *J. Phys. Chem.* **1966**, *70*, 2639−2659.

(44) Lobo, V. M. M.; Quaresma, J. L. *Handbook of Electrolyte Solutions*; Elsevier: Amsterdam, 1989.

(45) Sridharan, S.; Cukier, R. I. The mutual diffusion coefficient of a fluid in the presence of macroparticles. *J. Phys. Chem.* **1984**, *88*, 1237−1242.

(46) Annunziata, O.; Buzatu, D.; Albright, J. G. Effect of lysozyme proteins on the mutual-diffusion coefficient of sodium chloride in water. *J. Chem. Eng. Data* **2011**, *56*, 4849−4852.

(47) Branca, C.; Magazù, S.; Maisano, G.; Migliardo, F.; Migliardo, P.; Romeo, G. Hydration study of PEG/water mixtures by quasi elastic light scattering, acoustic and rheological measurements. *J. Phys. Chem. B* **2002**, *106*, 10272−10276.

(48) Annunziata, O. On the role of solute solvation and excluded-volume interactions in coupled diffusion. *J. Phys. Chem. B* **2008**, *112*, 11968−11975.

(49) Miller, D. G. Thermodynamics of irreversible processes. The experimental verification of the Onsager reciprocal relations. *Chem. Rev.* **1960**, *60*, 15−37.

(50) Record, M. T.; Anderson, C. F. Interpretation of preferential interaction coefficients of nonelectrolytes and of electrolyte ions in terms of a two domain model. *Biophys. J.* **1995**, *68*, 786−794.

(51) Timasheff, S. N. Protein hydration, thermodynamic binding, and preferential hydration. *Biochemistry* **2002**, *41*, 13473−13482.